



Contents lists available at ScienceDirect

Tunnelling and Underground Space Technology

journal homepage: www.elsevier.com/locate/tust

Trenchless Technology Research

A three-dimensional analysis of the effects of erosion voids on rigid pipes



Mohamed A. Meguid*, Sherif Kamel

Civil Engineering and Applied Mechanics, McGill University, 817 Sherbrooke Street West, Montreal, Quebec H3A 0C3, Canada

ARTICLE INFO

Article history:

Received 13 September 2011
 Received in revised form 26 October 2013
 Accepted 21 May 2014

Keywords:

Earth pressure
 Concrete pipes
 Erosion voids
 Finite element
 Pipe failure

ABSTRACT

In this study, elasto-plastic finite element analyses are performed to investigate the three-dimensional effects of erosion voids developing behind the walls of an existing sewer pipe on the earth pressure distribution around the pipe and the stresses in the pipe wall. Initial earth pressures are first calculated and compared with field measurements. Erosion voids of different sizes are then introduced at the springline and invert of the pipe and the changes in pressure are evaluated and compared with the initial values. The effects of increasing the void length, depth and angle are examined. Results clearly reveal that the presence of erosion voids can have a significant impact on the earth pressure distribution around an existing pipe as well as on the pipe wall stresses. Increase in pressure is found to be mainly influenced by the void length and location with respect to the pipe circumference. Voids introduced at the springline resulted in earth pressure increase of more than 100% near the void boundaries whereas the pressure change was less significant when the void is introduced at the pipe invert. The findings of this study highlight the importance of locating voids behind pipe walls to prevent further deterioration and possibly sewer failure.

© 2014 Elsevier Ltd. All rights reserved.

1. Introduction

Concrete pipes are used extensively for sanitary sewer, industrial discharge lines, culverts, and storm drains. These pipes are generally designed using either standard trench or embankment installation. The earth pressure acting on the pipe wall is usually calculated using various empirical (e.g. Marston and Anderson, 1913; Spangler and Handy, 1973), analytical (e.g. Burns and Richard, 1964; Hoeg, 1968), and numerical methods (e.g. Katona and Smith, 1976; Tohda et al., 1990) assuming full contact between the pipe and the surrounding soil. With time deterioration of the pipe-soil system and water leakage can result in local support loss due to loosening of the supporting material and, eventually, the development of erosion voids behind the pipe wall. In addition, improper construction procedure can accelerate the deterioration process, shortening the service life of the pipe and in some cases can lead to sudden failure. Talesnick and Baker (1999) reported the failure of a 1.2 m diameter concrete-lined steel sewage pipe buried in clayey soils. Field investigations revealed the formation of a physical gap of approximately 20 mm between the invert and the bedding layer. Severe cracking developed at the crown

and springline along a 300 m segment of the pipeline. Although the loss of soil support in the above example may not have been due to soil erosion, it illustrates the possible consequences of support loss around or under buried pipes.

Tan and Moore (2007) investigated numerically the effect of erosion voids on the wall stresses of rigid pipes using two-dimensional (2D) analysis. The influence of both the void size and location (e.g. springline and invert) on the stresses and bending moments developed in the pipe wall was investigated. Results of an elastic model showed that the presence of a void at springline leads to an increase in the extreme fiber stresses and the bending moments at all critical locations: crown, springlines and invert. The rate of increase was found to be controlled by the growth of the void in contact with the rigid pipe. Extending the model to include the shear failure effect of the soil resulted in stresses and moments higher than those reported in the elastic analysis. Changing the location of the void from springline to invert resulted in reduction in bending moment values followed by a reverse of the moment sign at crown, springlines and invert.

Meguid and Dang (2009) studied numerically the effect of void formation around an existing tunnel on the circumferential stresses in the lining. A series of elastic-plastic finite element analyses were carried out to investigate the effect of different parameters (e.g., flexibility ratio, coefficient of earth pressure at rest and void size) on thrust forces and bending moments in the lining. When

* Corresponding author. Tel.: +1 (514) 398 1537; fax: +1 (514) 398 7361.

E-mail addresses: mohamed.meguid@mcgill.ca (M.A. Meguid), sherif.kamel@mail.mcgill.ca (S. Kamel).

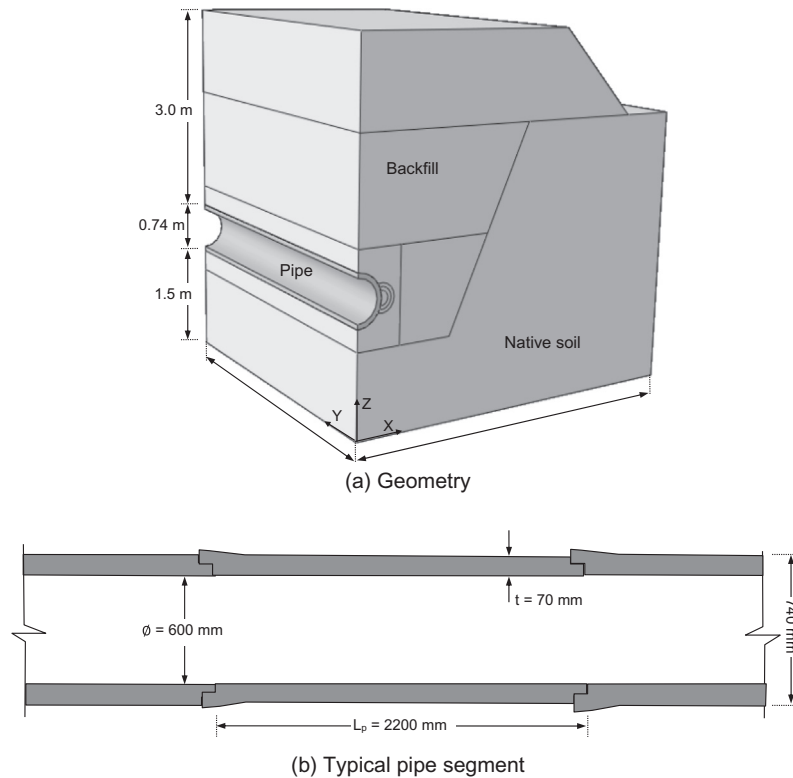


Fig. 1. Problem statement (a) geometry; (b) typical pipe segment (adapted from Liedberg, 1991).

the void was located at the springline, bending moment significantly increased. Similar results were reported for the thrust forces under the same conditions regardless of the flexibility ratio. The presence of erosion void at the lining invert was found to reduce the bending moments causing reversal in the sign of the moment as the void size increased.

Leung and Meguid (2011) conducted an experimental investigation to measure the changes in earth pressure around a tunnel lining due to the introduction of a local contact loss at different locations around the lining. The results showed that earth pressure increased locally around the separated section with a maximum increase of 25% at the springline.

The above studies illustrate the significant changes in earth pressure and internal forces in the walls of buried structures when the soil separates locally from the structure. However, these studies were limited to 2D models assuming that erosion void extends significantly along the wall of the buried structure.

The objective of this paper is to investigate the three-dimensional (3D) effects of erosion voids induced in the vicinity of the wall of a buried concrete pipe on the earth pressure distribution around the pipe and on the pipe wall stresses. Series of 3D nonlinear finite element analyses have been performed to investigate how a progressive increase in the void size affects the initial earth pressure acting on the pipe and the stresses in the pipe wall. The size and location of the induced voids have been varied and the corresponding pipe response has been calculated.

2. Problem statement

The investigated problem involves a concrete pipe 600 mm in inner diameter and 70 mm in wall thickness installed using the embankment installation method with 3 m soil cover above the crown. The pipe is first placed in a large trapezoidal shaped trench on a layer of bedding material and backfilled in layers and covered by an embankment. The problem geometry and material

properties used in this investigation were based on the full scale field tests carried out in an abandoned sand pit (Liedberg, 1991). The geological formation of site was reported to consist of a glaciofluvial delta built up of uniformly graded medium sand. This particular case study was chosen due to the availability of a complete set of soil and earth pressure data. The problem geometry showing the pipe location is shown in Fig. 1a. The dimensions of a typical pipe segment as reported by Liedberg (1991) are presented in Fig. 1b.

To simulate the presence of erosion voids around the existing pipe in 3D space, semi-cylindrical zones were predefined at specific locations next to the pipe wall assuming that voids will have a simplified circular geometry. The void sizes have been varied spatially in the x , y and z directions to reflect the effect of increasing the void depth, length, and angle, respectively. The voids were introduced at two locations around the pipe circumference, namely, springline and invert. The three parameters controlling the size of voids have been normalized. The void depth (V_D), length (V_L), and angle (V_A) have been normalized with respect to the mean pipe radius (R), segment length (L_p), and pipe circumference (2π), respectively, throughout the analysis. The above controlling parameters have been varied incrementally as summarized in Table 1.

Table 1
Parameters investigated.

Void angle (V_A) (°)	Void depth (V_D) (cm)	Void length (V_L) (cm)
31	2.5	20, 40, 60
	5	
	10	
47	5	
	10	
	15	
	20	
63	7.5	
	15	
	20	

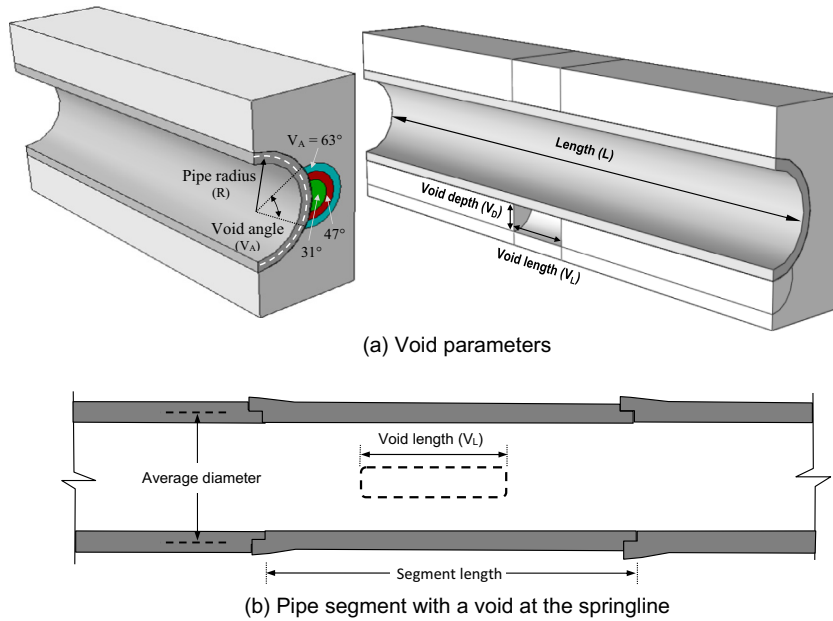


Fig. 2. A 3D schematic of the pipe with deteriorated soil (a) void parameters and (b) pipe segment with a void at the springline.

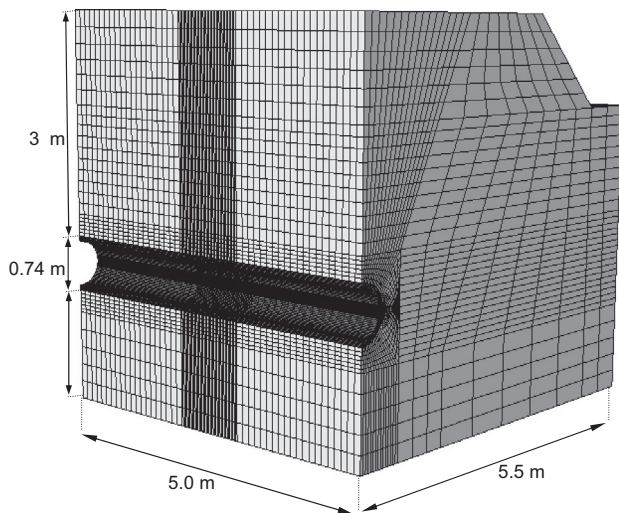


Fig. 3. A typical finite element mesh.

3. Numerical details

A total of eighteen (18) different models were built in this study including nine models for each void location (springline and invert). All models were solved using the general nonlinear finite element code ABAQUS version 6.9-1EF. Only half of the geometry is analyzed due to the symmetry of the problem. Both the pipe and the soil are modeled using solid elements C3D20 available in ABAQUS element library. These elements are general purpose quadratic brick elements with 20 nodes and 27 integration points. The elements can capture the stress concentration and is capable of modeling complex curved surfaces (ABAQUS, 2009) (see Fig. 2).

Table 2
Soil and pipe parameters.

	Density ρ (t/m ³)	Elastic modulus E (MPa)	Poisson's ratio ν	Friction angle ϕ (°)	Dilation angle ψ (°)	Cohesion c (kPa)	Plastic strain ϵ_p
Native soil	2.0	138	0.2	42.5	29.8	5	0
Backfill	1.7	2,274	0.34	39	27.5	5	0
Concrete pipe	2.6	34,000	0.2	–	–	–	–

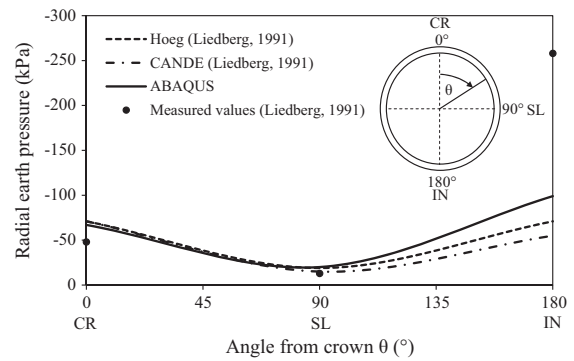


Fig. 4. Measured and calculated earth pressure distribution using different methods.

A parametric study was performed to determine the locations of the model boundaries that minimize the boundary effects on the stresses and displacements around the pipe. The model was restrained in the horizontal direction (i.e. smooth rigid) at the four vertical boundaries whereas the lower boundary was restrained in all three directions (i.e. rough rigid). A typical finite element mesh is shown in Fig. 3.

To account for the shear failure of the soil around the pipe, the soil was modeled using ABAQUS Mohr–Coulomb model, while, the concrete pipe was modeled using linear elastic material. The properties of the native soil located below the pipe and outside the trench were based on those reported by Liedberg (1991). The parameters used in modeling the pipe and the different soil layers are summarized in Table 2. A fully bonded interface between the pipe wall and the backfill material has been assumed. This was achieved by defining tie constraints at the pipe–soil interface

considering the pipe as the master-surface and the surrounding soil as the slave-surface.

Eleven steps were performed in each model to simulate the staged construction process. The model was first subjected to geostatic stresses with lateral earth pressure coefficient at rest ($K_0 = 1 - \sin \phi$) of 0.32. This was followed by the placement of both the pipe and the bedding layer and the activation of the soil-pipe interaction. Once the system equilibrium was reached, additional soil lifts were placed in stages to reach the target height of the embankment. After reaching the as-built condition, the erosion voids were introduced in three consecutive steps to reflect the void growth in the close vicinity of the pipe. Voids were simulated using the element removal technique where the stiffness of the eliminated elements was set to zero and these elements were gradually removed from the finite element mesh.

3.1. Model validation

To validate the model used in this study, the geometry and material properties reported by Liedberg (1991) were adopted and the earth pressure acting on the concrete pipe was calculated. The initial earth pressure results before voids were introduced are presented in Fig. 4 along with those reported by Liedberg (1991).

The calculated results at the crown ($\theta = 0^\circ$) and springline ($\theta = 90^\circ$) reasonably agreed with those measured and calculated using different methods. Pressures at the pipe invert ($\theta = 180^\circ$), however, varied even among the different numerical methods due to the sensitivity of the earth pressure to the backfill quality located at the pipe haunch. Since the actual field condition is hard to duplicate numerically depending on the software used in the analysis, ABAQUS results were found to differ from that reported using CANDE software. As the objective of this study is to compare the earth pressures on the pipe before and after introducing erosion voids, the initial pressures calculated are considered to be sufficient for the purpose of this investigation. It is worth mentioning that although the emphasis is placed in this study on the pipe response, given the soil properties ($c = 5$ kPa), shear failure was generally limited to small localized zones at the edge of the introduced voids.

4. Changes in earth pressure

To examine the effects of erosion voids on the earth pressure distribution around the investigated pipe, two different sets of graphs have been utilized. The first set includes transverse sections across the middle of the pipe and the second includes longitudinal

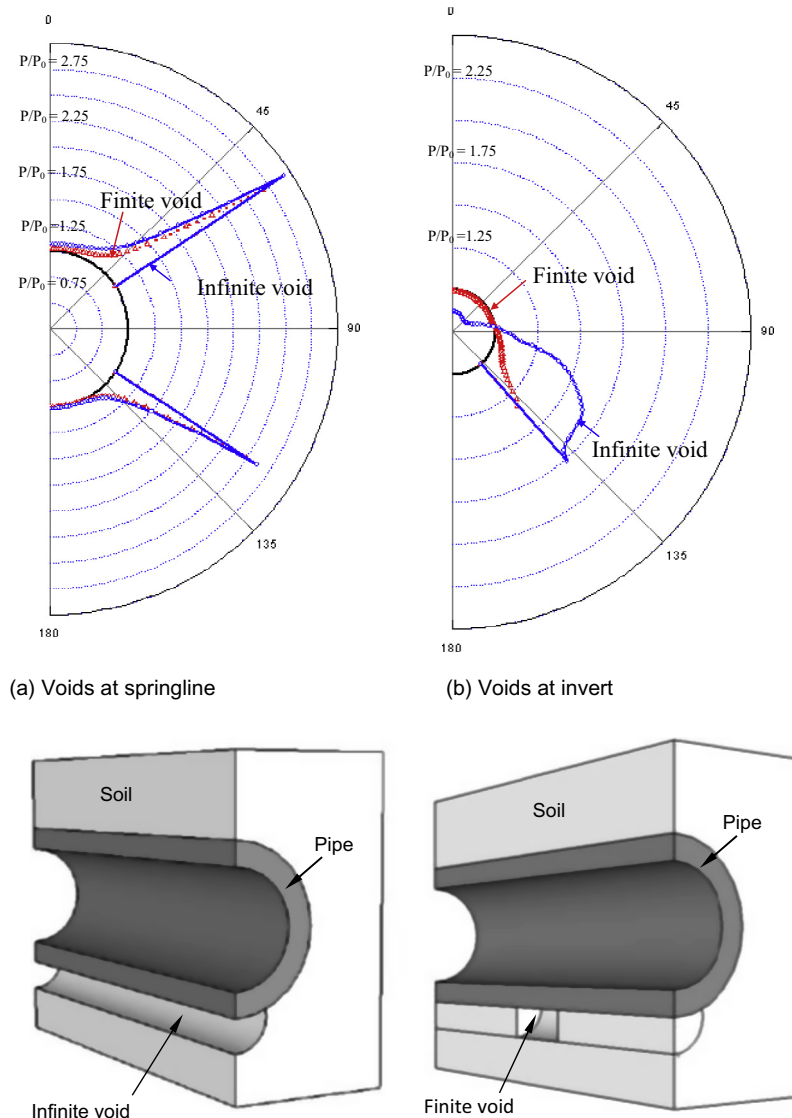


Fig. 5. Changes in earth pressure at section A–A for infinite and finite voids at (a) springline and (b) invert.

sections passing through the void boundary. The calculated earth pressures (P) are normalized with respect to the initial earth pressures (P_0) values throughout the study.

4.1. Transverse section of the pipe

The calculated changes in earth pressure at a transverse section due to void introduction are presented in Fig. 5(a) and (b) for the springline and invert, locations, respectively. The results compare the pressure distributions for both infinite and finite voids that make an angle, V_A , of 63° (or $V_A/2\pi = 17.5\%$). The introduction of a void next to the pipe wall has generally resulted in an increase in earth pressure locally around the void boundaries. It has been found that infinite voids resulted in higher earth pressure values as compared to finite voids at the same location. The increase in pressure reached about 40% when the voids were located at the invert. It should be mentioned that most erosion voids develop within a limited zone near the pipe wall and they are generally of limited extent along the pipe. Therefore, the rest of the results presented in this section will focus on the pipe response to finite voids.

Fig. 6(a) and (b) shows the changes in earth pressure calculated at a transverse section for two different void sizes (31° or $V_A/2\pi = 9\%$ and 63° or $V_A/2\pi = 17.5\%$). The earth pressure ratios (P/P_0)

P_0) are plotted on the radial coordinates whereas the angles from the pipe crown (in degrees) are plotted on the angular coordinates. In general, earth pressures increased sharply near the void boundaries and decreased to the initial values ($P/P_0 = 1$) at angles that range from 20 to 45 degrees in the radial direction depending on the void location. At the springline, the pressure ratio (P/P_0) increased to about 2.5 and decreased rapidly to the initial value at an angle of approximately 20° from the boundary (see Fig. 6a). Moving the voids to the invert (Fig. 6b) caused a maximum increase in earth pressure of about 1.25 times the initial values.

It is worth noting that the above results are in general agreement with those reported in the literature. The experimental investigation conducted by Leung and Meguid (2011) showed a significant increase in pressure at the springline compared to the changes measured at the invert. Tan and Moore (2007) and Meguid and Dang (2009) also confirmed that the presence of voids at the invert can lead to a reduction in the magnitude of bending moments developing in the pipe wall and reversal in the moment sign.

4.2. Effect of void length

The effects of void length on the changes in earth pressure along the pipe are shown in Figs. 7 and 8 for voids introduced at the springline and invert, respectively. The horizontal axis represents

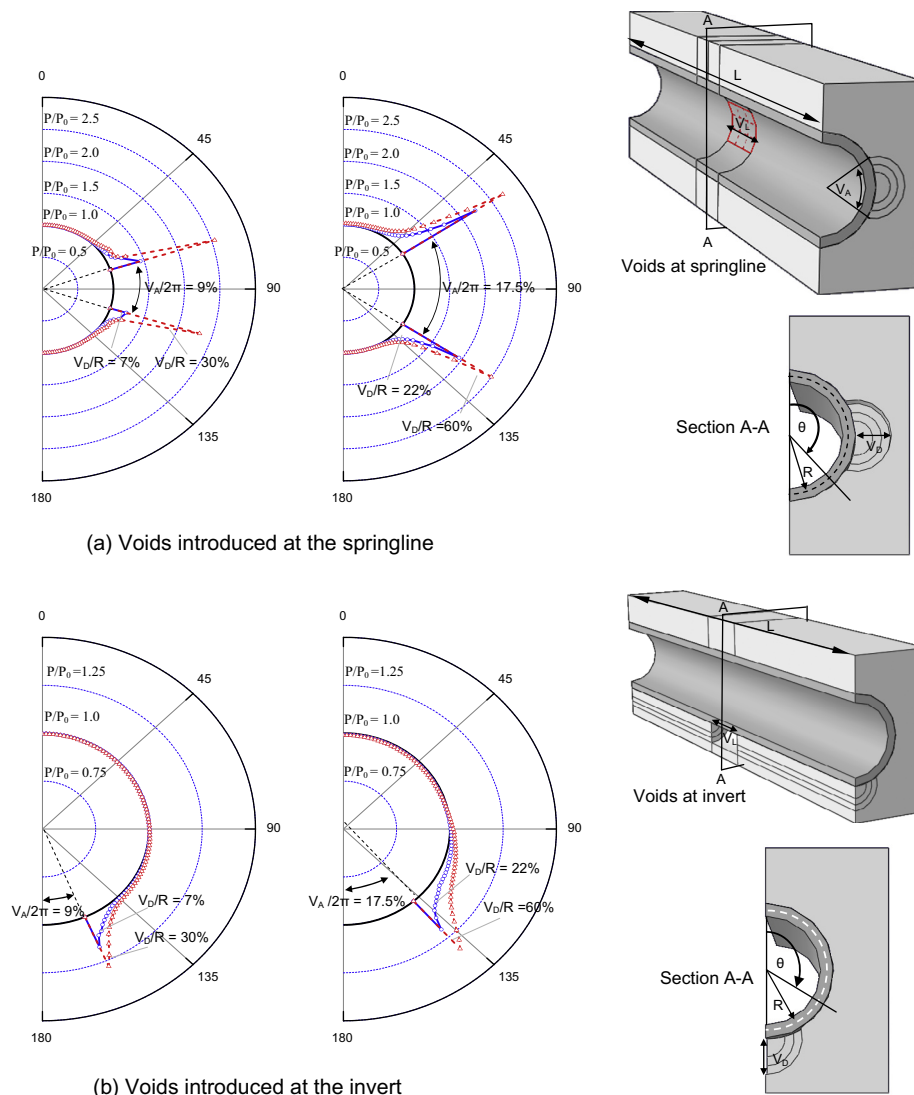


Fig. 6. Changes in earth pressure at section A-A for voids at (a) springline and (b) invert.

the normalized distance with respect to the pipe length (Y/L). The presented changes in earth pressure are for a void angle of 63° . For a given void depth, the earth pressure increased as the void length (V_L/L_P) increased. When the length of the void reached 27% of the length of the pipe segment, the earth pressure reached about 2.5 times the initial values. In all cases, the affected pipe length was found to be approximately 1 meter or 20% of the pipe length. By comparing the three plots in Fig. 7, it can be seen that the changes in void depth from 22% to 60% of the pipe radius led to slight increase in the maximum earth pressure calculated (about 0.6 times the initial values).

A similar trend was observed when the void was located at the invert as shown in Fig. 8. For a void angle of 63° , the increase in void length led to a general increase in earth pressure at the boundary. However, the pressure increase was found to be less significant compared to the springline condition with a maximum increase in pressure of about 1.3 times the initial values. It is also noted that the pressure decreased ultimately reached P/P_0 values

that are slightly higher than 1. This is attributed to the stress redistribution around the created void under the pipe and the non-deformable nature of the pipe.

An interesting finding that can be deduced from Figs. 7 and 8 is that the location of the erosion void can have a significant effect on the earth pressure distribution around the pipe. When the voids develop at the springline, earth pressure locally increases around the void boundaries to values that depend mostly on the length of the void. At the pipe invert, in addition to the local pressure increase at the void boundaries, the earth pressures slightly increase along an extended length of the pipe. This is in agreement of what has been found by Tan and Moore (2007).

A summary of all results related to the effect of void length is shown in Fig. 9. An increasing trend can be seen at both the springline and invert locations. The increase in pressure at the springline ranged from 25% (for void angle 31°) to approximately 45% (for void angle 63°) whereas the corresponding increase at the invert ranged from 20% to 30%.

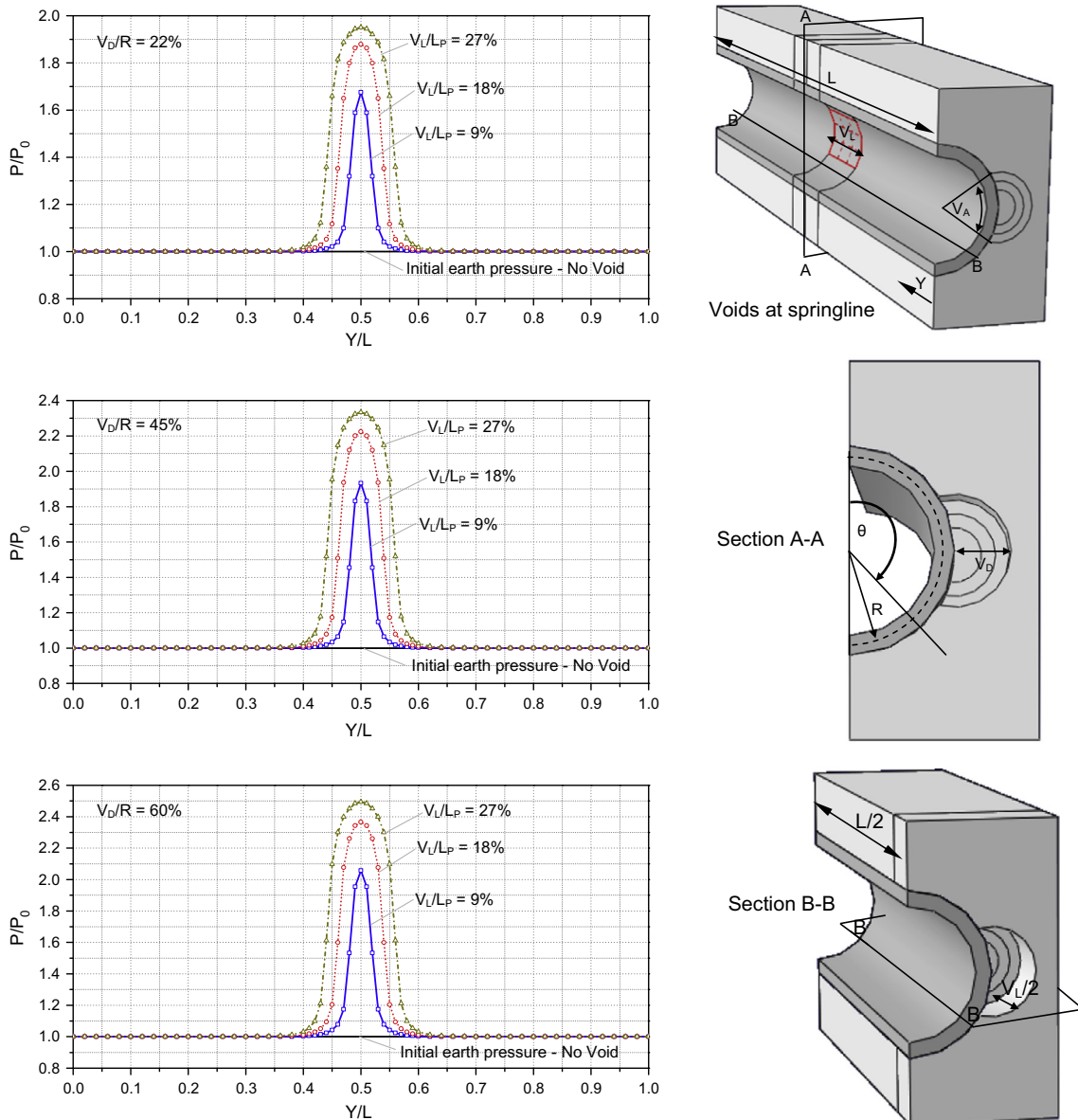
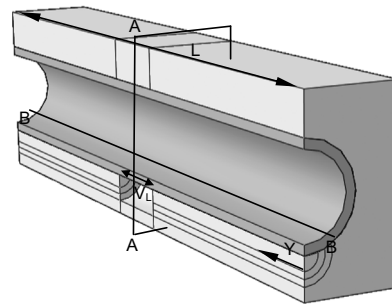
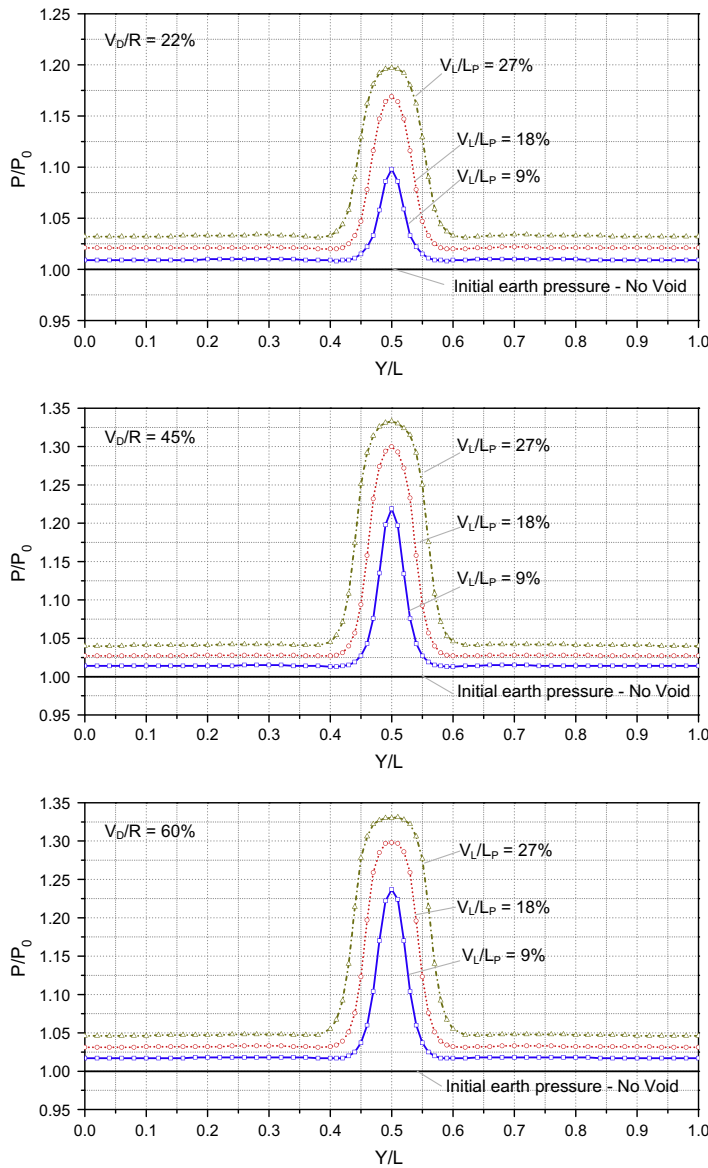
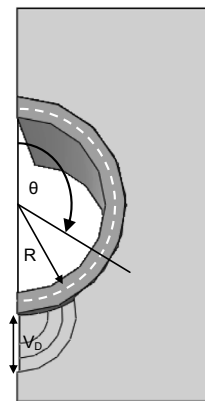


Fig. 7. Effect of void length on the changes in earth pressure along the pipe for voids at the springline.



Voids at invert & Section B-B



Section A-A

Fig. 8. Effect of void length on the changes in earth pressure along the pipe for voids at the invert.

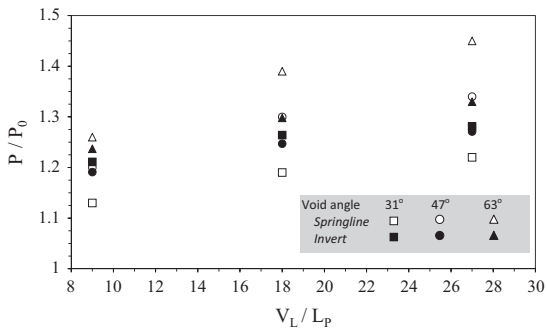


Fig. 9. Effect of void length on the changes in earth pressure.

4.3. Effect of void depth

Figs. 10 and 11 show the effect of void depth (V_D) on the changes in earth pressure at the void boundary. The results are presented for a void angle of 63° and three different void lengths ($V_L/L_p = 9\%$, 18% , and 27%). For a given void length, increasing the void

depth (V_D/R) was found to slightly increase the contact pressure along the boundary. The increase in pressure reached a maximum value of about 40% of the initial pressure and decreased rapidly with distance from the void.

Similar behavior was found for voids located at the pipe invert as shown in Fig. 11. The maximum pressure increase was found to be about 15% of the initial values. Fig. 11 also shows that increasing the void depth to radius ratio from 45% to 60% of the pipe radius did not cause additional increase in pressure. Fig. 12 shows a summary of the calculated results at the springline and invert emphasizing the effect of void depth on the earth pressure represented by P/P_0 ratio. It is evident from the figure that for a given void angle increasing the void depth causes a consistent increase in earth pressure with more increase at the springline compared to the invert.

4.4. Effect of void angle

Fig. 13 presents the relationship between the normalized void angle ($V_A/2\pi$) and the earth pressure ratio (P/P_0) for the investi-

gated range of parameters (void length of 60 cm and the corresponding void depths of each angle as defined in Table 1). The earth pressure was found to increase at both the springline and invert with the increase in the normalized void angle. The maximum increase in earth pressure reached about 40% at the springline and about 30% at the pipe invert.

5. Changes in pipe stresses

5.1. Changes in bending moments

In order to investigate the effect of erosion voids on the ring moments in both the circumferential and longitudinal directions, two different sets of graphs have been utilized. The first includes the moments calculated at a transverse section (A–A) across the middle of the pipe as presented in Fig. 14. The second set includes the moments calculated at longitudinal section (B–B) passing through the springline of the pipe as presented in Figs. 15 and

16, respectively. Bending moments were calculated using the approach described by Munro et al. (2009) as follow:

$$1/\rho = (\varepsilon_1 - \varepsilon_2)/t$$

where $1/\rho$ is the change in pipe curvature, ε_1 and ε_2 are the inner and outer circumferential strains, respectively and t is the pipe wall thickness.

The moment can then be calculated as follows:

$$M = E_p I_p / \rho$$

where E_p is the pipe modulus and $I_p = t^3/12$ is the second moment of area of the pipe cross section.

In Fig. 14, the calculated moments M_0 are presented on the horizontal axis and the angle from the pipe crown θ on the vertical axis. The results are presented for (a) the springline and (b) the invert voids with length of 60 cm and normalized void angle that ranged from 9% to 17.5%. It can be seen that voids at the springline led to local increase in moment at the void location coupled with small decrease in moment at the crown and invert

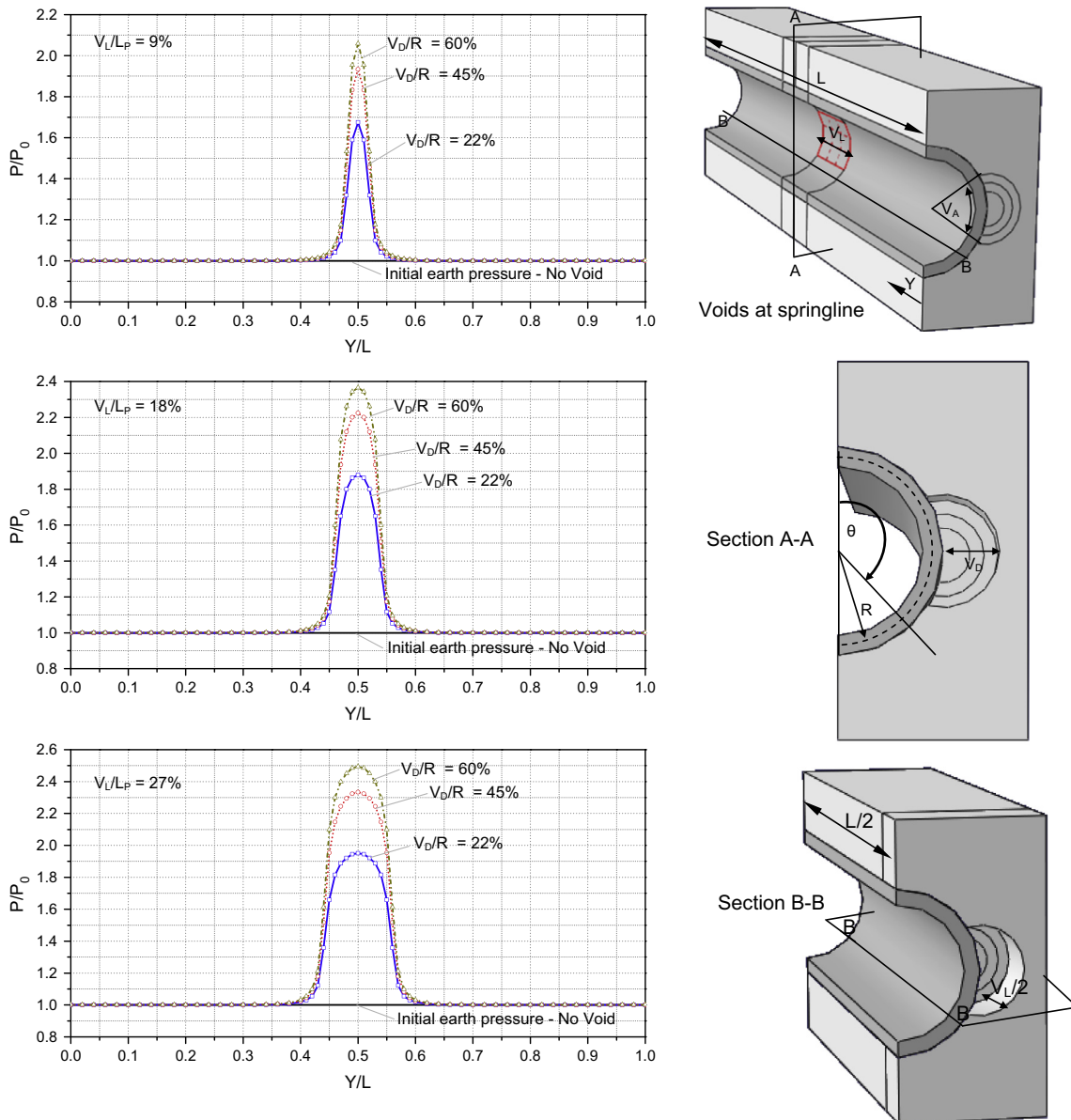


Fig. 10. Effect of void depth on the changes in earth pressure along the pipe for voids at the springline.

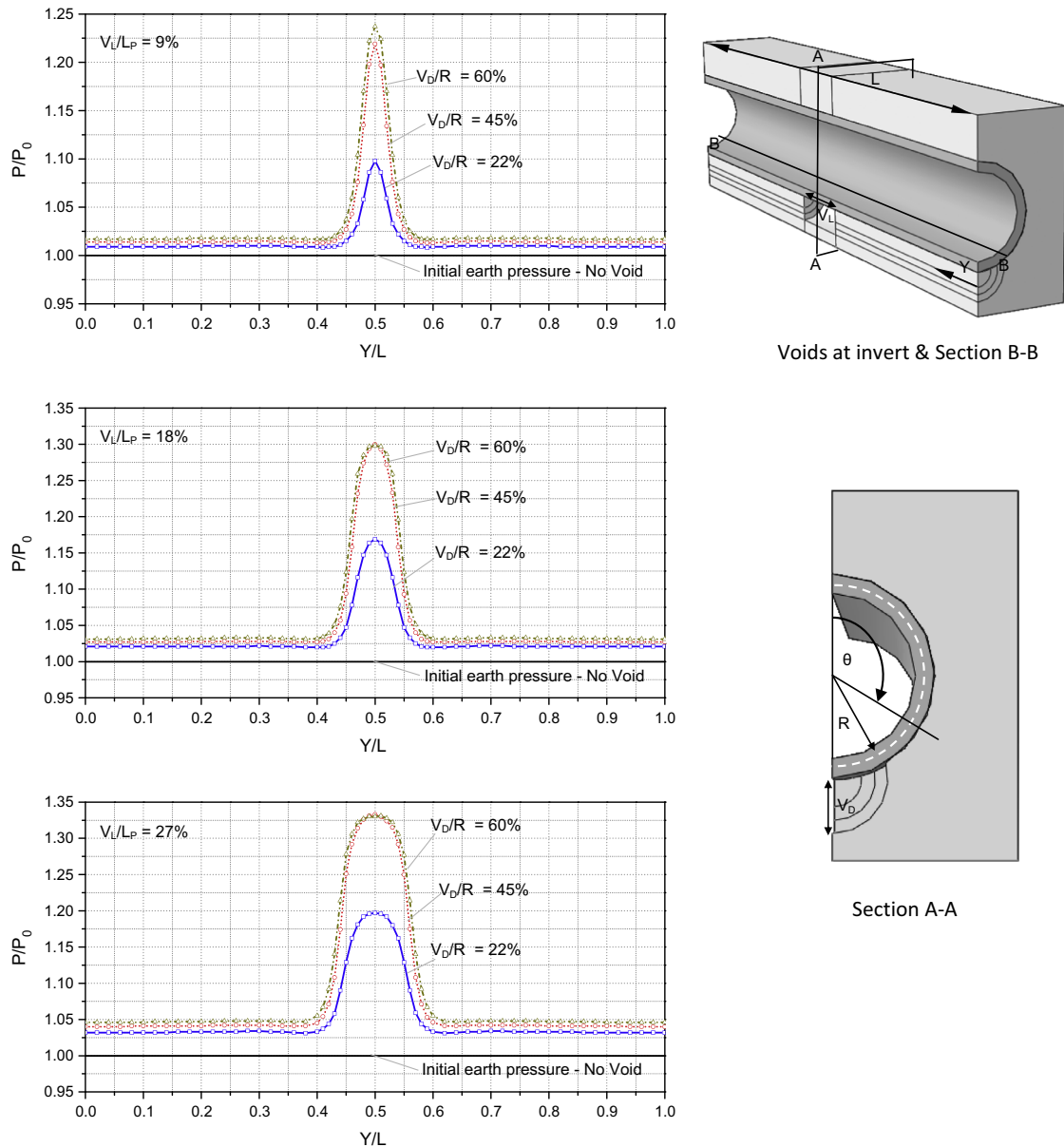


Fig. 11. Effect of void depth on the changes in earth pressure along the pipe for voids at the invert.

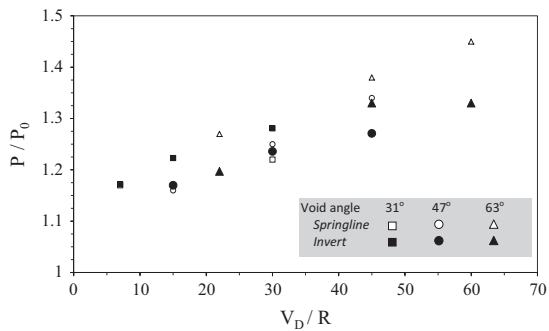


Fig. 12. Effect of void depth on the changes in earth pressure.

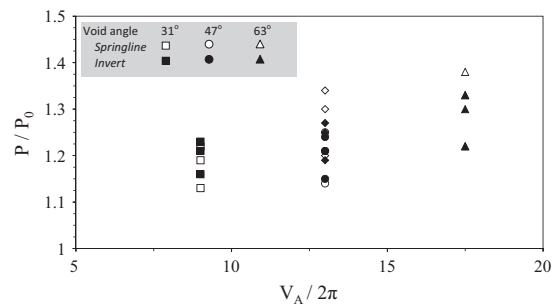


Fig. 13. Effect of void angle on the changes in earth pressure.

(Fig. 14a). The moment increase was calculated to be about 40% (from about -1.4 to -1.7 kN m/m). On the other hand, at the pipe invert (Fig. 14b), a local decrease in moment from about 1.4 – 0.6 kN m/m was calculated. The moment decrease in the circum-

ferential (ring) direction at the invert location can be explained by the tendency of the moment to reverse sign from compression (positive) to tension (negative) as a result of the support loss within the void area.

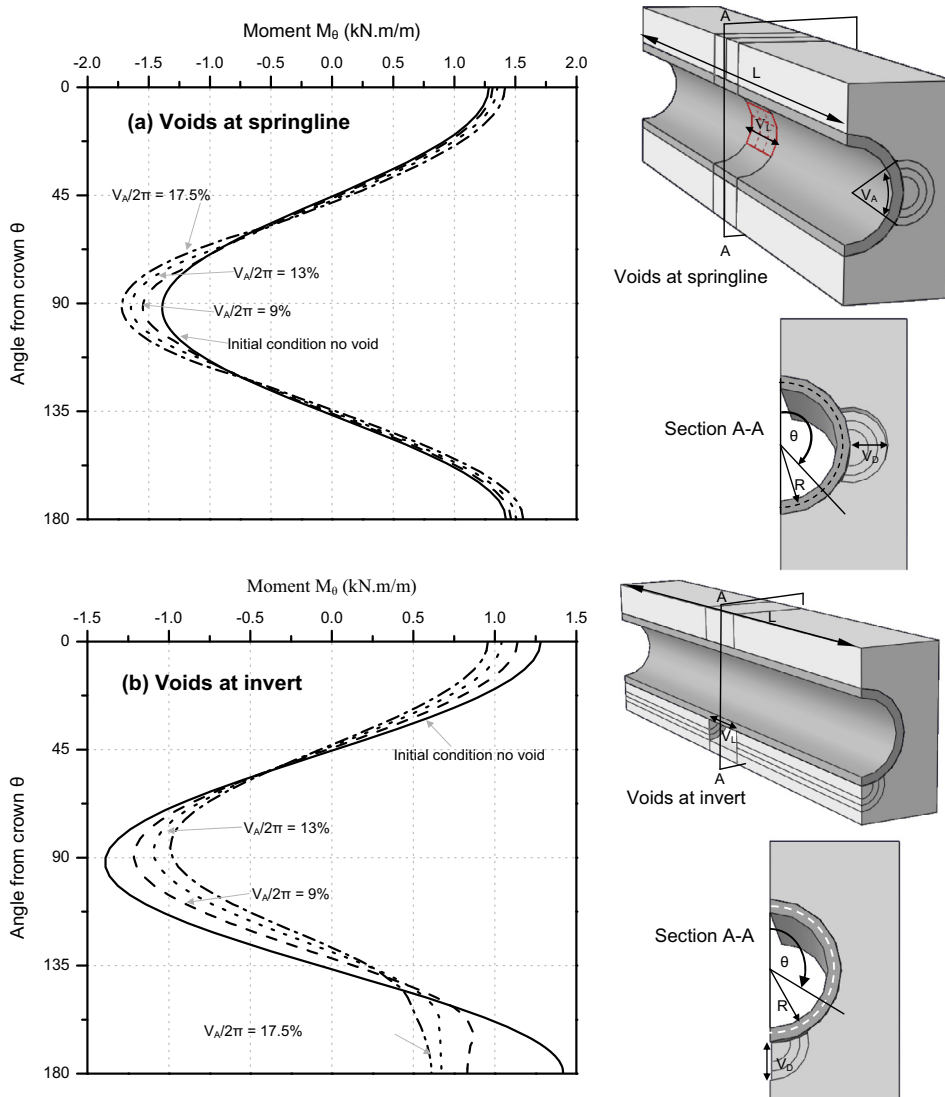


Fig. 14. Calculated ring moments when voids are introduced at (a) the springline and (b) the invert.

For the same void sizes, the percentage change in ring moments calculated along the pipe length at the crown, springline and invert locations are plotted versus the normalized pipe length (Y/L) and presented in Figs. 15 and 16 for voids at the springline and invert, respectively. For voids at the springline, an increase in moment of 24% was calculated at the springline, while the increase at the crown and invert reached a maximum value of about 10% (see Fig. 15). For voids at the invert (Fig. 16), a maximum reduction in bending moments of $-60%$, $-30%$ and $-25%$ were calculated at the invert, springline and crown, respectively. In all cases, the affected pipe length is approximately 2.5–3 m which corresponds to about 5 times the void length.

5.2. Changes in circumferential stresses at the extreme fibers of the pipe wall

Stresses at the extreme fibers of the pipe presented in this section are calculated using the inner and outer strains determined at the nodes as indicated in Section 5.1. The effects of increasing the void size on the changes in tensile and compressive stresses are presented in Figs. 17 and 18, respectively. In these figures, the percentage change in tensile and compressive stress is presented on the vertical axis at the crown, springline and invert. The results presented are calculated at section A–A (shown in Fig. 16) for three

different void angles ($V_A/2\pi = 9%$, $13%$, and $17.5%$) when the voids reached their maximum length of 60 cm ($V_L/L_P = 27%$) and void depths as defined in Table 1. In general, there is a consistent increase in tensile stresses at all investigated locations as the void angle increases. At the springline, a maximum increase in tensile stress of about 36%; while the reduction in tensile stress is about 55% for voids at the invert (see Fig. 17). Fig. 18 shows that compressive stress increased about 18% for voids at the springline with a maximum decrease of 65% for voids at the invert.

5.3. Changes in longitudinal stresses at the outer fiber of the pipe wall

The effect of increasing the void length on the changes in longitudinal stresses is presented in Figs. 19 and 20 for voids introduced at the springline and invert, respectively. The results presented are calculated at section A–A (shown in Fig. 18) at the extreme outer fiber for three different void angles ($V_A/2\pi = 9%$, $13%$, and $17.5%$), when the voids reached their maximum depths, as specified in Table 1.

The presence of voids at the springline and invert resulted in two different behaviors. At the springline, consistent increase in tensile stresses is calculated as the void size increased. The rate of stress increase in the longitudinal direction is found to be significant (up to 80%) as compared to that calculated in the circumfer-

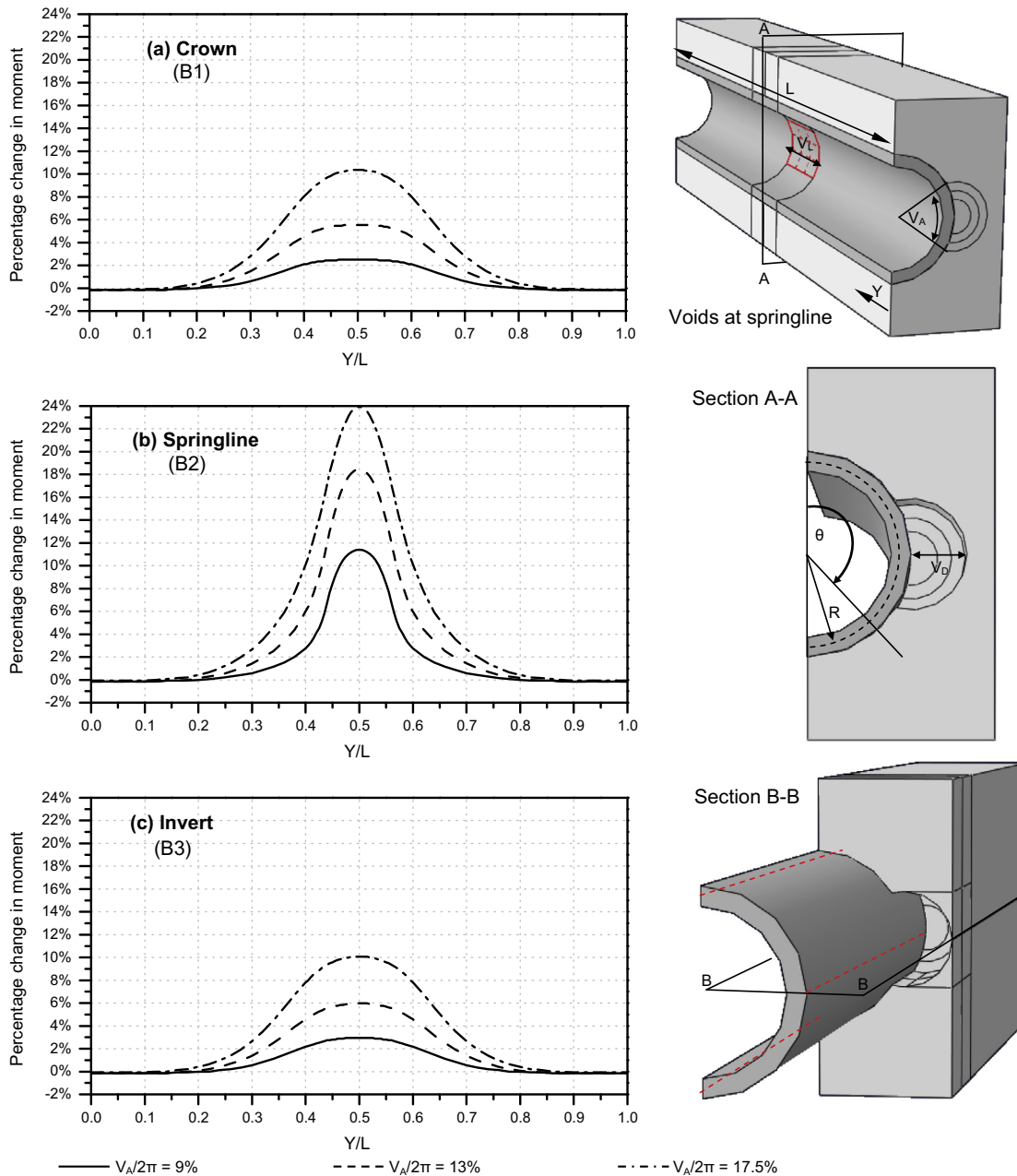


Fig. 15. Percentage change in ring moment along the pipe calculated at (a) crown, (b) springline and (c) invert for voids at the springline.

ential direction. For voids at the invert, the increase in void size resulted in a reduction in the calculated compressive stresses. With further growth in void size the stresses at the invert switched from compressive to tensile in the longitudinal direction with a maximum increase in tensile stresses of about 125%. Therefore, the presence of voids at the invert can be critical particularly for non-reinforced concrete pipes.

6. Summary and conclusions

Three-dimensional nonlinear finite element analyses have been performed to examine the impact of erosion voids located behind the wall of a concrete pipe in 3D space on the changes in earth pressure and wall stresses in the pipe wall. Voids were introduced at two locations; namely, the springline and invert and for each case different void angles, depths and lengths were examined. The changes in stresses were calculated at a transverse section as

well as along the pipe length. The conclusions arising from the analysis are as follow:

6.1. Changes in earth pressure

- (1) It has been found that the changes in earth pressure took place at the void boundaries. For voids located at the springline, earth pressure increased by more than 100% of the initial values. Less significant changes were found when the voids were located at the invert with a maximum earth pressure of about 30%.
- (2) The void location and length (along the pipe axis) are key factors affecting the changes in earth pressure. Less effect was found when the void depth increased from about 20% to 60% of the pipe radius, particularly for voids located at the invert. Similarly, the void angle was found to slightly affect the earth pressure distribution at the pipe invert.

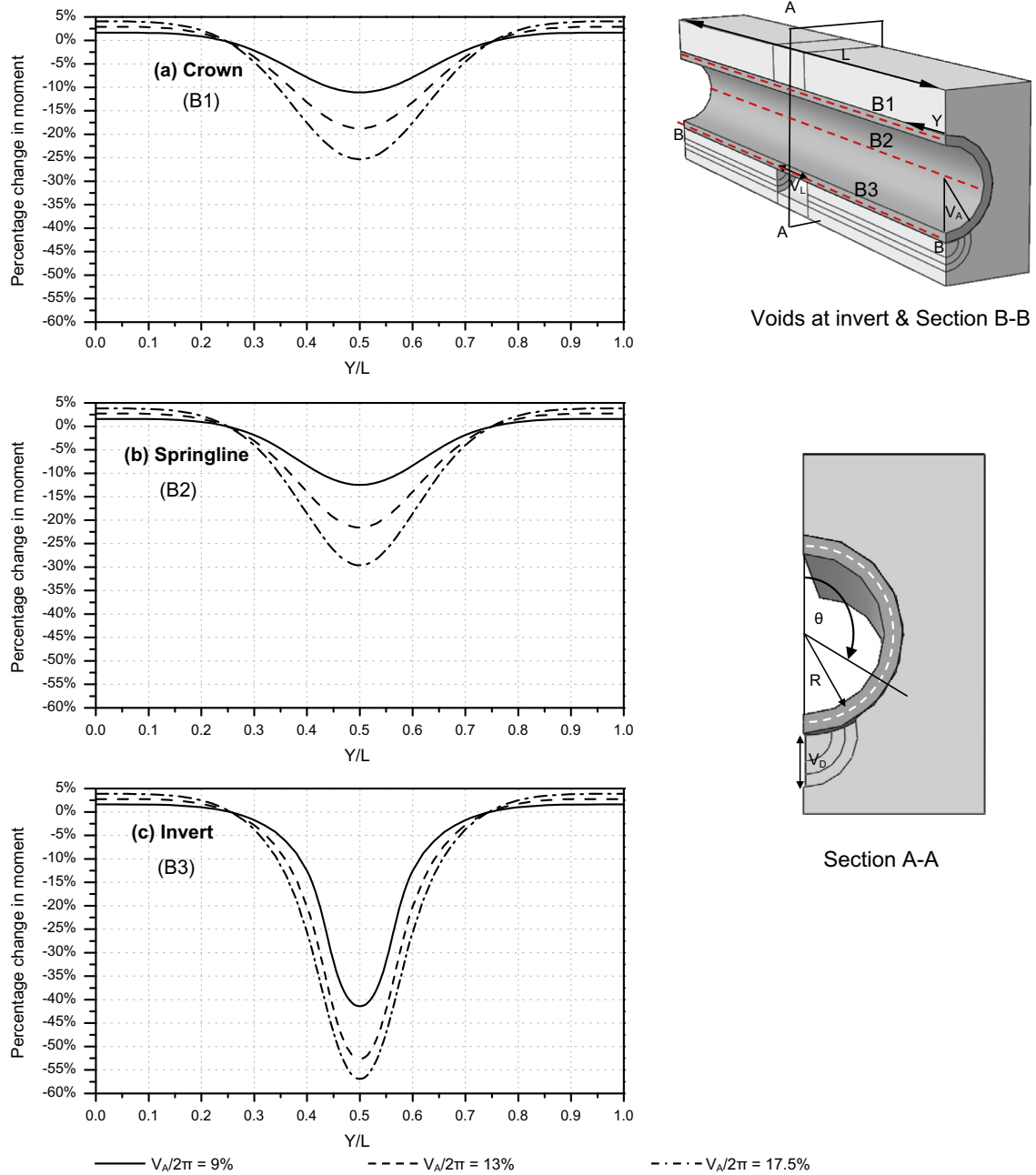


Fig. 16. Percentage change in ring moment along the pipe calculated at (a) crown, (b) springline and (c) invert for voids at the invert.

6.2. Changes in pipe stresses

- (1) It has been found that areas in the close vicinity of the voids experienced the highest changes in wall stresses.
- (2) The presence of the voids at the springline resulted in an increase in the pipe stresses and bending moments. Different behavior has been noted for voids introduced at the invert where a reduction in stresses and moments was calculated.
- (3) The maximum increase in tensile stresses in the circumferential direction was found to be about 36% for voids introduced at the springline; when the voids were moved to the invert, a maximum reduction of 65% was calculated.

- (4) Significant changes in longitudinal stresses were generally found at the outer fiber of the pipe. At the springline, the initial tensile stresses increased by about 80% whereas at the invert, the initial compressive stresses switched sign leading to a total change of about 225%.

It should be noted that a factor of safety ranging from 1.25 to 1.5 is typically used in the design of concrete pipes (ACPA, 2007). Coupling this design criterion with the findings of this research indicates that the development of erosion voids under the invert of rigid pipes is the most critical condition. As illustrated above, if tensile stresses developing at the invert increase to a level greater than the pipe capacity, the ultimate tensile strength of the concrete will be exceeded leading to crack initiation at the pipe

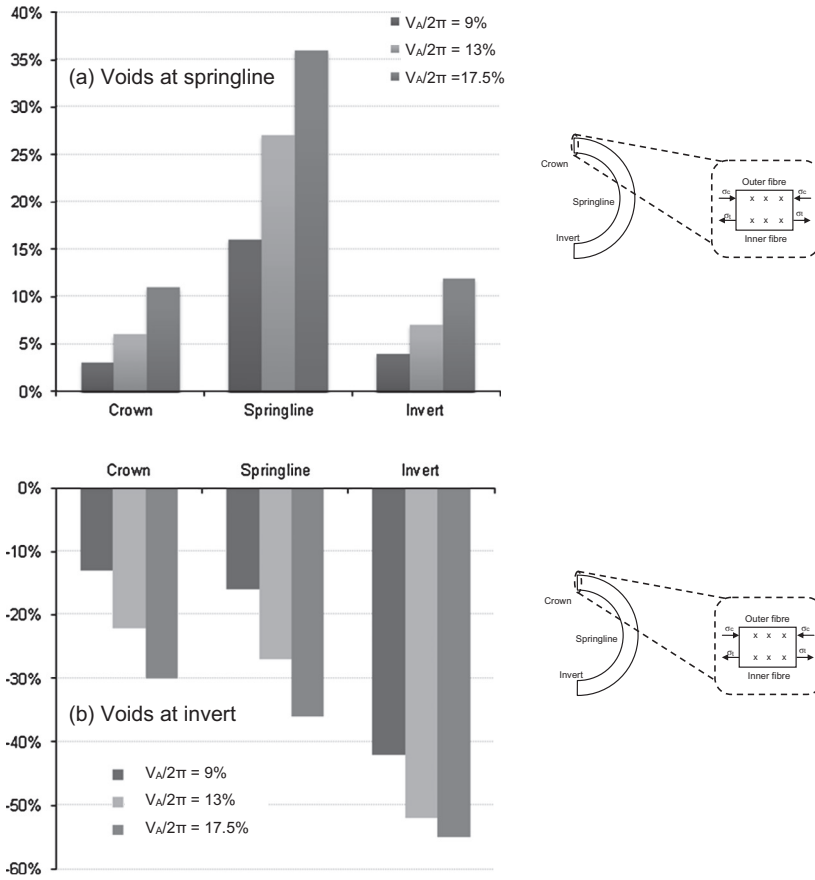


Fig. 17. Percentage change in maximum tensile stresses calculated at crown, springline and invert for voids introduced at (a) springline and (b) invert.

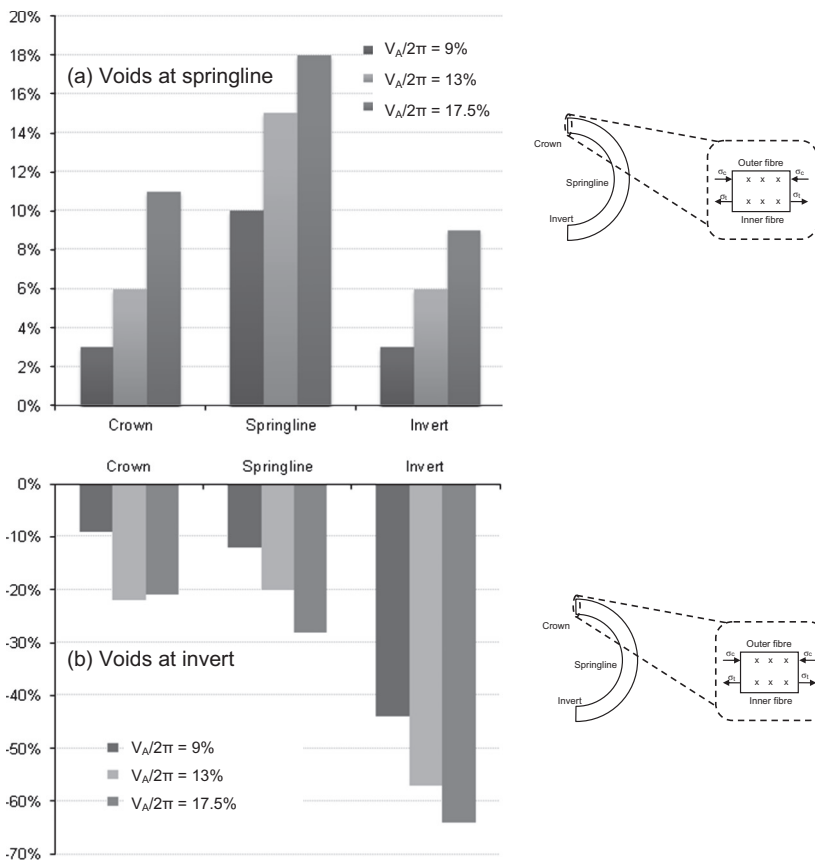


Fig. 18. Percentage change in maximum compressive stresses calculated at crown, springline and invert for voids introduced at (a) springline and (b) invert.

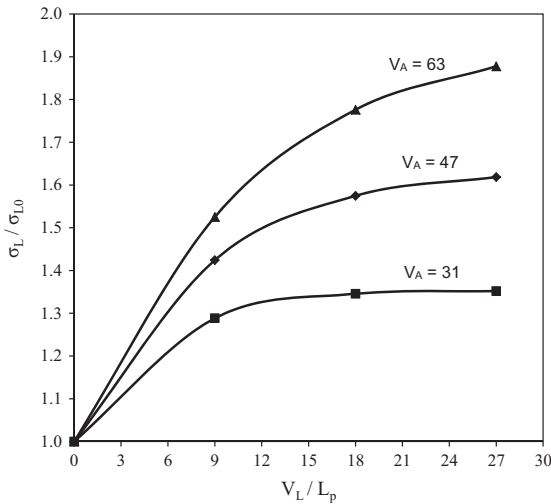
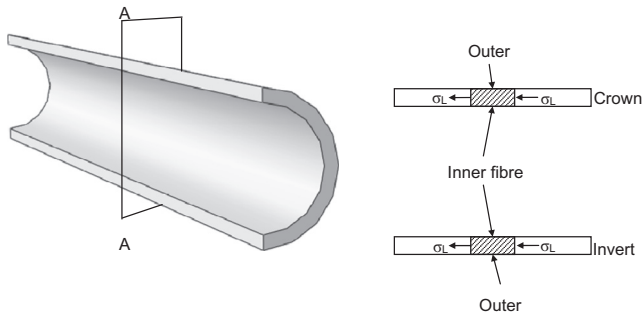


Fig. 19. Changes in longitudinal stresses at extreme outer fiber for voids at springline.

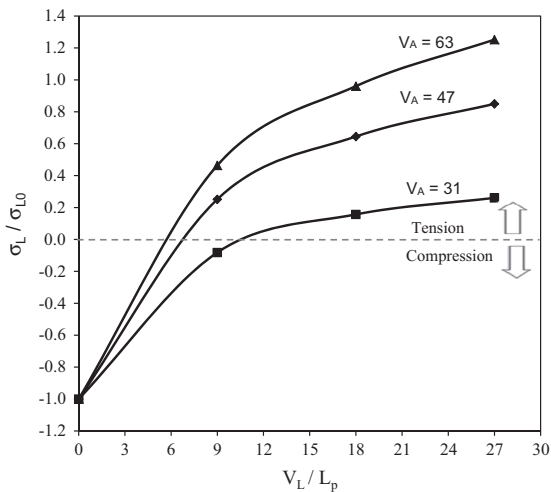
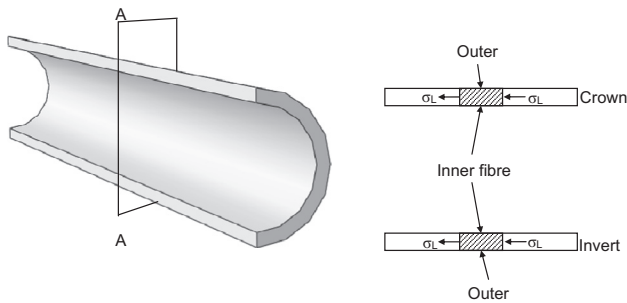


Fig. 20. Changes in longitudinal stresses at extreme outer fiber for voids at invert.

invert. This local overstressing in the pipe material can be accelerated by further softening and erosion of the supporting soil.

The findings of this study suggest that the presence of erosion voids can significantly change the earth pressure distribution and the stresses in the pipe wall. The progressive increase in void size should be avoided by early detection and treatment of the affected area.

Acknowledgement

This research is supported by the Natural Sciences and Engineering Research Council of Canada (NSERC) under Grant Number 311971-06.

References

ABAQUS, Standard User's Manual, vols. I & II, 2009. Hibbit, Karlsson & Sorensen Inc., Pawtucket, Rhode Island.

ACPA, 2007. Concrete Pipe Design Manual. American Concrete Pipe Association.

Burns, J.Q., Richard, R.M., 1964. Attenuation of stresses for buried cylinders. In: Proceedings, Symposium of Soil-Structure Interaction, Arizona University, pp. 378–392.

Hoeg, K., 1968. Stresses against underground structural cylinders. In: American Society of Civil Engineers Proceedings. J. Soil Mech. Found. Div. 94 (SM4), 833–858.

Katona, M.G., Smith, J.M., 1976. Modern approach for structural design of culverts. IPC Sci. Technol. Press, Ltd., Guildford, Surrey, England, pp. 128–140.

Leung, C., Meguid, M.A., 2011. An experimental study of the effect of local contact loss on the earth pressure distribution on existing tunnel linings. *Tunn. Undergr. Space Technol.* 26 (1), 139–145.

Liedberg, S., 1991. Earth pressure distribution against rigid pipes under various bedding conditions. Full-Scale Field Tests in Sand, Chalmers Tekniska Hogskola, Doktorsavhandlingar, vol. 796, pp. 1–223.

Marston, A., Anderson, A.O., 1913. The theory of loads on pipes in ditches and tests of cement and clay drain tile and sewer pipe. Iowa State College of Agriculture, 181p.

Meguid, M.A., Dang, H.K., 2009. The effect of erosion voids on existing tunnel linings. *Tunn. Undergr. Space Technol.* 24 (3), 278–286.

Munro, S.M., Moore, I.D., Brachman, R.W.L., 2009. Laboratory testing to examine deformations and moments in fiber-reinforced cement pipe. *J. Geotech. Geoenviron. Eng.* 135 (11), 1722–1731.

Spangler, M.G., Handy, R.L., 1973. Soil Engineering. Intext Educational Publishers, New York.

Talesnick, M., Baker, R., 1999. Investigation of the failure of a concrete-lined steel pipe. *Geotech. Geol. Eng.* 17 (2), 99–121.

Tan, Z., Moore, I.D., 2007. Effect of backfill erosion on moments in buried rigid pipes. In: Transportation Research Board Annual Conference, Washington, DC.

Tohda, J., Mikasa, M., Hachiya, M., Nakahashi, S., 1990. FE elastic analysis of measured earth pressure on buried rigid pipes in centrifuge models. In: Pipeline Design and Installation: Proceedings of the International conference, Las Vegas, NV, USA, pp. 557–571.